REPORT DOCUMENTATION PAGE

Form Approved
OMB No. 0704-0188

1. REPORT DATE *(DD-MM-YYYY)*	**2. REPORT TYPE**	**3. DATES COVERED** *(From - To)*
08-08-2013	Final	06-15-2010 to 06-14-2013

4. TITLE AND SUBTITLE

Linking Tribofilm Nanomechanics to the Origin of Low Friction and Wear

5a. CONTRACT NUMBER
FA9550-10-1-0295

5b. GRANT NUMBER
FA9550-10-1-0295

5c. PROGRAM ELEMENT NUMBER

6. AUTHOR(S)

David L. Burris

5d. PROJECT NUMBER

5e. TASK NUMBER

5f. WORK UNIT NUMBER

7. PERFORMING ORGANIZATION NAME(S) AND ADDRESS(ES)

University of Delaware

8. PERFORMING ORGANIZATION REPORT NUMBER

9. SPONSORING / MONITORING AGENCY NAME(S) AND ADDRESS(ES)

Air Force Office of Scientific Research

10. SPONSOR/MONITOR'S ACRONYM(S)

AFOSR

11. SPONSOR/MONITOR'S REPORT NUMBER(S)

12. DISTRIBUTION / AVAILABILITY STATEMENT

Unclassified unlimited

13. SUPPLEMENTARY NOTES

14. ABSTRACT

Solid lubricants are required in applications where traditional lubricants are precluded by challenging environmental conditions (e.g. space). However, the mechanisms that enable low friction and low wear sliding of these systems remain poorly understood. Recent studies have demonstrated low friction sliding is consistently accompanied by nanoscale tribo-films whose properties and contributions to friction reduction are unknown. The goal of this study was to elucidate the role of nanoscale tribofilms in friction and wear reduction by correlating macroscale tribological properties with the results of in-situ measurements of transfer film morphology, chemistry, and nanomechanical properties. The materials included molybdenum disulfide (MoS2) and polytetrafluoroethylene (PTFE), two very different but well studied and heavily used solid lubricants known for exceptional tribological characteristics. The tools used for the study included in-situ optical microscopy (morphology), interferometry (topography), and lateral force microscopy (tribology). A significant portion of the work was the development of a lateral force microscopy (LFM) calibration technique to enable quantitative and in-situ LFM measurements.

15. SUBJECT TERMS

Friction, transfer films, nanomechanics, solid lubricants

16. SECURITY CLASSIFICATION OF:			**17. LIMITATION OF ABSTRACT**	**18. NUMBER OF PAGES**	**19a. NAME OF RESPONSIBLE PERSON**
a. REPORT	**b. ABSTRACT**	**c. THIS PAGE**	UU		**19b. TELEPHONE NUMBER** *(include area code)*
UU	UU	UU			

Executive Summary

Linking Tribofilm Nanomechanics to the Origins of Low Friction and Wear

Prof. David L. Burris
Mechanical Engineering Department, University of Delaware

HISTORICAL TRIBOLOGICAL MODELS have utilized bulk material properties to understand general tribological phenomena. There have been major successes with traditional materials whose motion accommodation mechanisms largely involve bulk deformation mechanics, but little is understood of the low friction and low wear mechanisms of systems that do not experience gross deformation or wear. ***The overall goal of the work was to develop the in-situ tools and methods to interrogate the tribological, morphological, and mechanical evolutions of tribological surfaces.***

During the course of the project, several tools were developed to elucidate mechanisms of solid lubrication. The project culminated in six primary accomplishments. First, a quantitative means for characterizing nanoparticle dispersion was developed to support nanomaterials synthesis. Second, an *in-situ* instrument was developed for optically tracking transfer films during sliding. Third, an *in-situ* calibration technique was developed to enable quantitative friction coefficient measurements with standard Atomic Force Microscopes. Fourth, a technique was developed to quantify transfer film morphology for correlation to friction and wear. Fifth, a microtribometer with environment and temperature control was developed to characterize tribological properties and develop transfer films in the range of aerospace relevant conditions. Sixth, a joint technical session on *in-situ* measurements was organized for the Nanotribology and Materials Tribology technical committees at the 2011 annual meeting of the Society of Tribologists and Lubrication Engineers and has become a recurring joint session. ***The project resulted in the following publications, submissions, or manuscripts in preparation:***

1) **A Quantitative Method for Measuring Nanocomposite Dispersion,** H.S. Khare, D.L. Burris, *Polymer* 51 (2010) 719-729.
2) **Characterization of nanoscale surface films in solid lubricants,** H.S. Khare, D.L. Burris, Tribology and Lubrication Technology, May 2012
3) **Methods in characterization of nano-scale friction in solid lubricants**, H.S. Khare, D.L. Burris, Tribology and Lubrication Technology, September 2012
4) **Transfer film evolution and its role in promoting ultra-low wear of a PTFE nanocomposite,** J. Ye, H.S. Khare, D.L. Burris, *Wear 1-2 (2013) 1095-1102*
5) **The extended wedge methd: Atomic force microscope friction calibration for improved tolerance to instrument misalignments, tip-offset, and blunt probes,** H.S. Khare, D.L. Burris, *Review of Scientific Instruments 84 (2013) 055108*
6) **The effects of environmental water and oxygen on the temperature dependent friction of sputtered molybdenum disulfide,** H. Khare, D.L. Burris, *In review by Tribology Letters*
7) **Surface and sub-surface contributions of oxidation and moisture to ambient temperature friction of molybdenum disulfide,** H. Khare, D.L. Burris, *in preparation for Tribology Letters*
8) **Quantifying transfer film quality,** J. Ye, H. Khare, D.L. Burris, *in preparation for Wear*
9) **Micro- and nanomechanical properties of transfer films from alumina-PTFE nanocomposites,** J. Ye, D.L. Burris, *in preparation for Wear*

David L. Burris, Ph.D. was the principle investigator on the project. Harman S. Khare, B.S., and Jiaxin Ye, M.S. carried out the experimental work on the project for their anticipated doctoral degrees.

Final Report

Linking Tribofilm Nanomechanics to the Origins of Low Friction and Wear

Prof. David L. Burris
Mechanical Engineering Department, University of Delaware

1.0 Introduction

1.1 Broad Impacts of Tribological Challenges

Technological advancements in air and space technology depend upon comparable advancements in our ability to control tribological performance in increasingly demanding conditions. Recently developed nanostructured materials with novel wear resistance are uniquely suited for fundamental studies of friction and provide a foundation for the design of low friction, low wear materials for use in extreme applications.

Tribology-derived engineering challenges are vast and span a diverse spectrum of technologies with national and global implications. The feasibility of a variety of green and sustainable energy sources hinges on the development of advanced lubrication strategies for improved friction and wear management. For example, increased size and power output of wind turbines reduce specific costs, but also contribute to stresses and temperatures that exceed the capabilities of existing gearbox lubrication technology [1]. Gearbox reliability is a major barrier to wind power and is the focus of the NREL initiated Gearbox Reliability Collaborative [2].

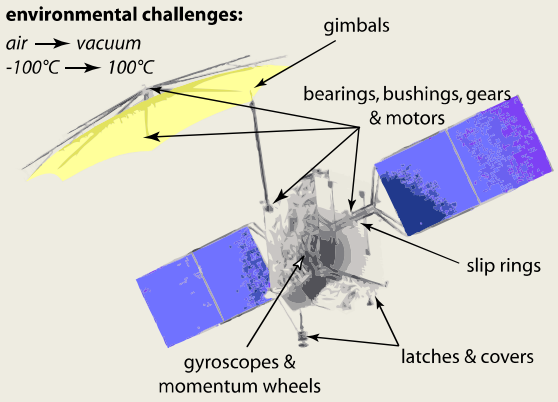

Figure 1. A typical space satellite illustrating numerous mission critical tribological elements and the associated environmental challenges.

The lubrication needs of the Air-Force range from the extremely high temperatures of jet exhaust thrusters to the cryogenic hard-vacuum conditions experienced by satellites. The conditions of space are almost singularly challenging. The combination of hard-vacuum, thermal extremes, radiation and atomic oxygen is exceptionally damaging and there are continued efforts to simply understand the static degradation of materials exposed to this environment [3, 4]. Space-bound resources of the air-force have a wide variety of moving parts that are responsible for deployment, positioning, power management, data collection and communication during flight. The execution of these mission critical tasks hinges entirely on the ability of the solid lubricant to survive and perform reliably in damaging contact and environmental conditions; new materials are needed to address the tribological challenges presented by the operational demands of the Air Force [5, 6].

1.2 State of the Art in Space Lubrication and Tribo-Materials Design

It is extremely challenging to provide effective and reliable lubrication in space. Traditional lubricants evaporate in the absence of environmental pressure. Inert, low vapor pressure

fluorinated greases are robust, but migrate (flow) from the contact with time and experience large viscosity fluctuations in varying thermal environments. In general, solid surfaces adhere strongly in the absence of adsorbed surface contaminants and often 'cold weld' in vacuum if not properly lubricated [5]. Any surface that may encounter contact during space flight must be protected by an adhesion resistant coating.

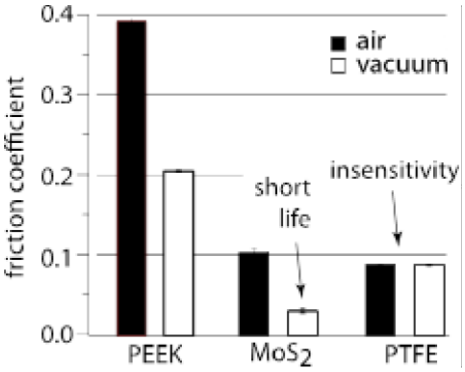

Figure 2. Unpublished friction coefficient data for PEEK, MoS_2 and PTFE in air and vacuum (10^{-5} torr). Interestingly, while both polymers are chemically inert, PEEK was found sensitive, while PTFE was not. Reports of environmental sensitivity of friction are common, but the responsible mechanisms are unclear.

Molybdenum disulphide (MoS_2) is a lamellar solid that has demonstrated unusually low friction and adhesion in hard vacuum as demonstrated in Figure 2. Consequently it has been widely used as a space coating. However, MoS_2 presents other engineering challenges. First, wear and friction increase with exposure to the water vapor of terrestrial conditions (Figure 2). Assembly, testing, transportation and launch vibrations on Earth can reduce life or fail the coating prior to deployment; the Galileo high gain antenna failure is thought to have been the result of an MoS_2 coating failure during transportation [6]. There have been a number of recent efforts to design 'adaptable' MoS_2-based solid lubricants to combat the tribological sensitivity of MoS_2 to ambient water vapor [7-13].

Wear is yet another challenge presented by these materials. MoS_2 has little bulk integrity and is only useful as a thin film that is typically on the 1 μm size-scale. Coating life is limited for these thin films even during sliding at very low wear rates (volume loss per unit normal load per distance slid). Additionally, the bond interface is susceptible to fatigue failure; this failure mode is speculated to have contributed to the Galileo failure [6].

There are significant research efforts to address the challenges of existing tribo-materials with developments of new coatings and bulk solid lubricants [8, 10, 13-23]. Several successful examples have demonstrated excellent performance in the laboratory and were involved in the first space-flight tribo-tests aboard the Materials International Space Station Experiment (MISSE 7). There is a wide array of applications where the physics governing the behavior of interest are well enough understood to enable the design of new materials for a limited set of physical properties (*e.g.* composites, alloys, heat treatments, etc.). Unfortunately, a lack of understanding of the governing physics of friction and wear has prevented tribo-material ***design*** from a ***predictive*** standpoint.

Fundamental studies targeting the origins of friction and wear are inherently difficult to conduct. Our relatively poor fundamental understanding of tribological phenomena and inability to design new materials has left scientists with only inherently inefficient iterative routes for materials discovery. This Edisonian approach to design is becoming intractable; our materials toolbox contains a wide array of modern materials from polymers to ceramics and manufacturing

techniques from atomic layer deposition to sol-gel synthesis. There are seemingly endless permutations of techniques, materials and properties available for use by a designer. Without guidance from models rooted in the fundamentals of friction and wear, the demands of future technologies will quickly outpace materials development capabilities.

1.3 Fundamental Studies in Tribology

A lack of fundamental understanding of the processes that govern friction and wear has prevented predictive design of tribological solids to date. Sliding interfaces involve coupled and complex chemical and physical processes, and scientists are persistently challenged by an inability to directly probe buried interfaces.

One of the first attempts to observe and correlate microscopic interfacial events to the macro-tribological response occurred over 50 years ago. Archard and Hirst used stylus profilometry to track features on a tagged segment of a metal surface during periods of mild and severe wear [24] as shown on the left of Figure 3.

In a similar, but modernized effort, Sawyer *et al*. (University of Florida) tracked wear over an area of interest using a scanning white-light interferometer (SWLI) with nanometer resolution (unpublished). Results for two extreme cases are depicted on the right of Figure 3. At the beginning of a control experiment with self-mated stainless steel, contaminant films from the environment protected the surfaces, and low friction coefficients (μ~0.2) and low wear rates were observed. However, after fewer than 10 cycles, dramatically increased friction coefficients accompanied the appearance of micrometer deep scratches in the wear track as the mating

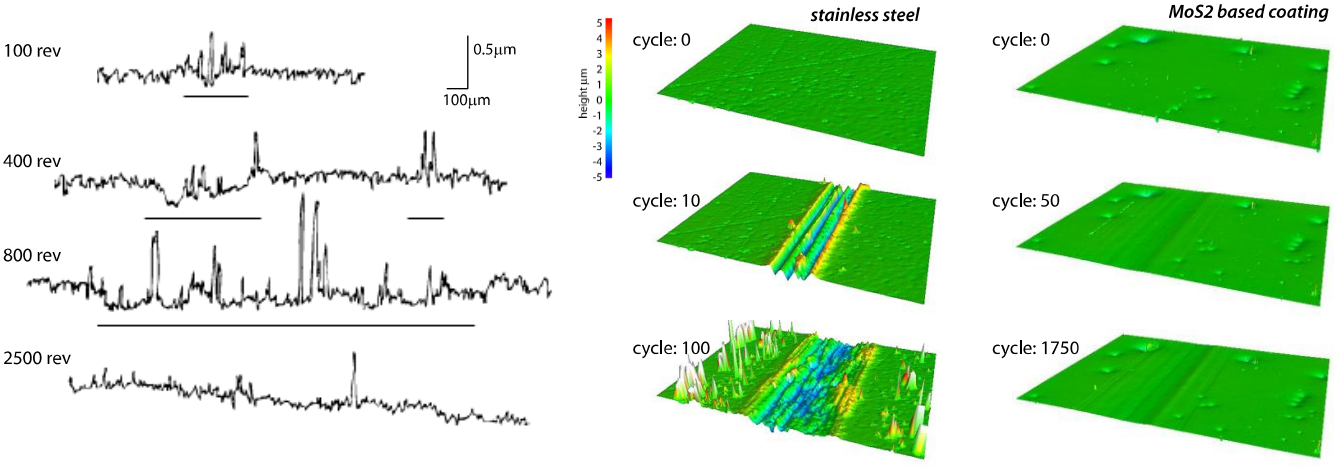

Figure 3. Left: A pioneering effort to quantitatively track topography during wear by Archard and Hirst [24]. The widths of the tracks as measured optically are shown under each record; peaks from material transfer of the micron size-scale are observed in the contacting areas. Right: Similar unpublished measurements by Sawyer *et al.* (unpublished) using a modern SWLI with stainless steel and an MoS_2 base coating. Strong adhesion of the stainless steel results in elevated friction and severe wear. The MoS_2 surface immediately responds to the applied stress and adapts to promote interfacial sliding through unclear mechanisms.

surfaces developed regions of strong adhesion. Following this point in the experiment, the tribo-system continued to deteriorate, and by cycle 100, the friction coefficient increased to $\mu > 0.6$ and debris particles littered the field-of-view.

In a follow-up experiment, an MoS_2-based coating was applied to the stainless steel substrate to prevent direct contact between the mating components. The coating reduced friction coefficients to $\mu < 0.1$ and, as shown by the interferometry measurements, successfully prevented gross deformation and adhesive wear. A 100 nm deep wear scar, which developed during transient sliding over the first 50 cycles, was visually identical at the conclusion of the 2,000 cycle experiment. Despite the visual lack of evidence of wear, the low steady-state wear rate of $4x10^{-8}$ mm^3/Nm was measurable via a combination of high measurement resolution and stable sample indexing.

'Observations' of buried interfaces have become less difficult with modern advancements in instrumentation; there have been recent efforts to more directly probe and observe interfacial processes *in-situ* using SEM/TEM [25] (AFRL), Raman spectroscopy [26-28], light microscopy and interferometry (unpublished University of Florida). These studies have provided strong evidence in favor of tribo-film interfacial sliding as the dominant velocity accommodation mode in candidate solid lubricants.

2.0 Research Objectives and Approaches

Recent studies have demonstrated that the nanoscale tribo-films that accompany low friction and wear [25, 29, 30] are highly ordered [31-34] and chemically altered [35] variants of the bulk. Although the mechanical properties of these films are also likely to be highly modified, they have not been well-characterized to date. These films are intimate at the tribological contact and it is hypothesized that the unique properties of interfacial tribo-films will prove to have a significant detectable impact on the tribological response of the system. ***The overall goal of the work was to develop the in-situ tools and methods to interrogate the tribological, morphological, and mechanical evolutions of tribological surfaces.*** The approach taken involved the use of PTFE, an exceptional bulk solid lubricant, and MoS_2, the most widely used solid lubricant in aerospace applications. During this project, a number of *in-situ* or quasi-*in-situ* methods were developed to characterize the tribological, morphological, chemical, and mechanical evolutions during tribological contacts.

3.0 Research Outcomes

3.1 Characterizing nanoparticle dispersion

Nanoparticle reinforcement is an extremely effective means for converting a poor tribological material into an outstanding solid lubricant. For example, trace loadings of alumina are known to reduce the wear of PTFE by four orders of magnitude [16, 36]. According to Burris *et al.* [37] in a recent review article on polymeric solid lubricants, the inability to quantitatively characterize filler dispersion makes it extremely difficult to link results of independent studies

and is among the primary barriers to advancement of our understanding of wear and friction reduction mechanisms of these materials. One of the first efforts in this project was the development of a quantitative filler dispersion characterization tool.

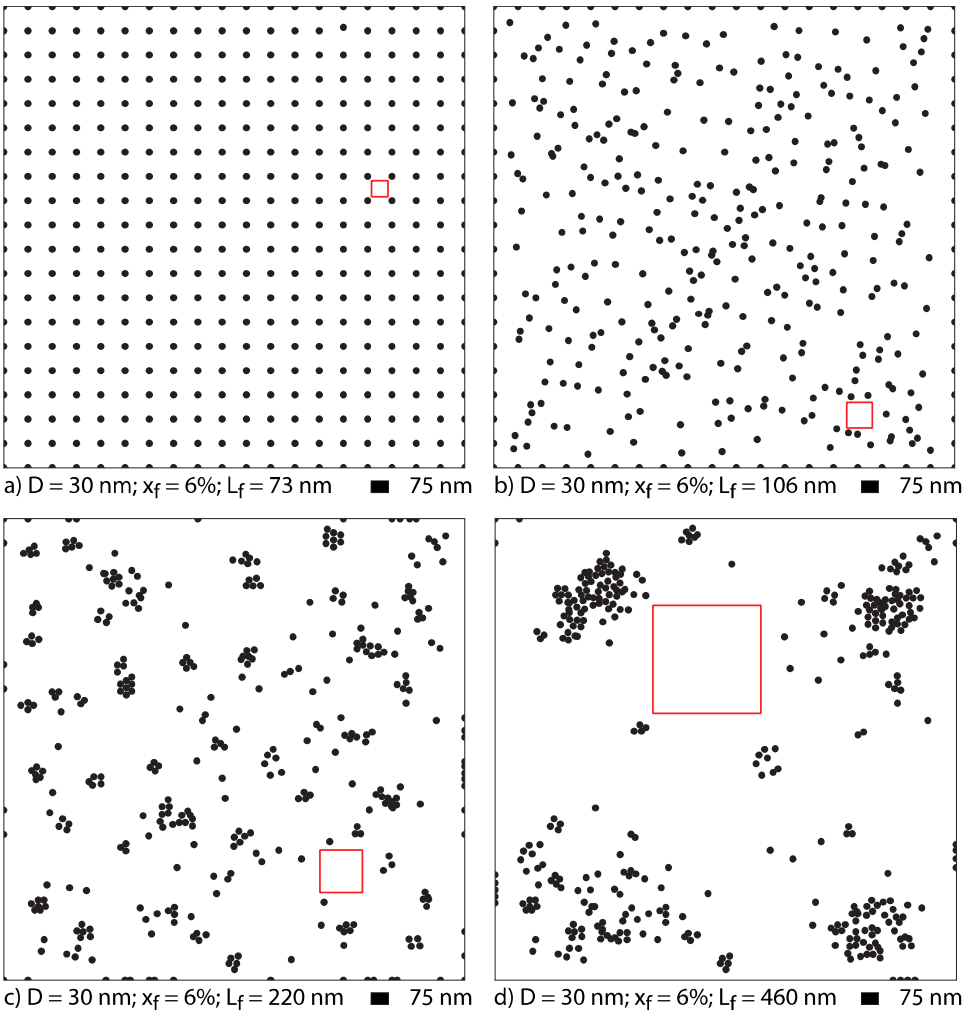

Figure 4. Varying dispersions of 30 nm particles at 6% loading a) uniform dispersion - L_f = 73 nm; b) random dispersion - L_f = 106 nm; c) clustered dispersion - L_f = 220 nm; d) agglomerated dispersion - L_f = 460 nm. Open squares have a length equal to the free-space length which increases as the dispersion worsens.

The concept is intuitive: the reinforcement of the polymer by the particle is a function of the characteristic size scale of the regions devoid of filler. This concept is consistent with the assumed benefits of nanoparticles over microparticles and uniform dispersions over agglomerated dispersions. This concept also simplifies the task of quantification; while there are infinite ways to quantitatively describe the distribution of particles, determination of the characteristic size of the unreinforced regions is relatively well-defined.

The fictitious images in Figure 4 illustrate varying dispersions of a nanocomposite with 6% 30 nm fillers. When these particles are randomly dispersed as shown in Figure 4b, the Poisson's

distribution can be used directly to determine the largest window for which the most probable number of intersecting particles is zero; in this case, the window has a length of 108nm. This window is defined here as the "free-space length", L_f. The Poisson's distribution cannot be used for real distributions. For arbitrary dispersions, a numerical Monte Carlo approach was adopted. Cross-sectional images of the composite are first converted to black and white, with black representing filler and white representing polymer. A Matlab™ script was written to automatically carry out the analysis. To numerically identify the free-space length, boxes of a specified size are randomly located over the image and the number of intersecting filler pixels is counted for each randomly placed box. The code iterates on the box size until it finds the largest box for which the most probable number of intersecting filler pixels is zero. The Matlab™ code and instructions for use are available on the PI's website at: **http://research.me.udel.edu/~dlburris/software/dispersion.html**. The free-space length is illustrated in Figure 4 for different dispersions of the same nanocomposite. The free-space length increases as the dispersion worsens, as the filler size increases, and as the filler loading decreases; thus the free-space length is consistent with general reinforcement strategies.

3.2 Quantifying transfer films

3.2.1 Morphology

Transfer film quality is widely implicated in the friction and wear reduction of successful solid lubricant materials, but no method has been established as an acceptable means of assessing transfer film quality. According to a recent review article on solid lubricants tribology [37], the lack of a quantitative metric of transfer film evaluation is one of the primary barriers to advancement in our understanding of solid lubricants tribology. One objective of this study was the development of a quantitative metric of transfer film quality that correlates to tribological performance.

The first challenge was to identify the features that correlate to tribological performance. Polymeric materials were targeted for this part of the project due to their prevalence in literature discussions of transfer films. An optical microscope was used to make quasi-*in-situ* measurements of transfer film morphology during a standard reciprocating wear experiment with a PTFE nanocomposite [38].

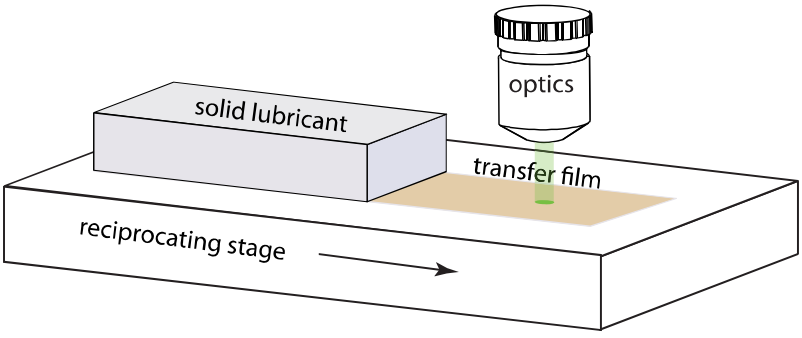

Figure 5. Schematic of in-situ transfer film characterization strategy. An optical microscope was used to evaluate transfer film morphology throughout the wear tests.

The measurements revealed marked changes in transfer film morphology throughout the life of the contact. Further, these morphological features were strongly correlated to the wear behavior of the solid lubricant. In the early stages of sliding, transfer films were thick and consisted of large poorly adhered platelets that were removed every time the pin passed. The wear rate was about an order of magnitude lower than unfilled PTFE and of the same order of magnitude as many unlubricated materials. During this period, the size of the platelets reduced monotonically with the wear rate until an abrupt transition occurred. At the transition, neither debris nor mass loss was detectable. However, an extremely thin film was detected with electron microscopy in this regime and consisted of ~100nm domains of PTFE-rich fragments that remained well-adhered for the rest of the experiment. After a period of no-wear sliding, small optically detectable fragments began to transfer; these fragments initiated the steady state transfer film, which had an island-like morphology and gave low but detectable wear rates. The morphologies in these three regimes are illustrated in Figure 6.

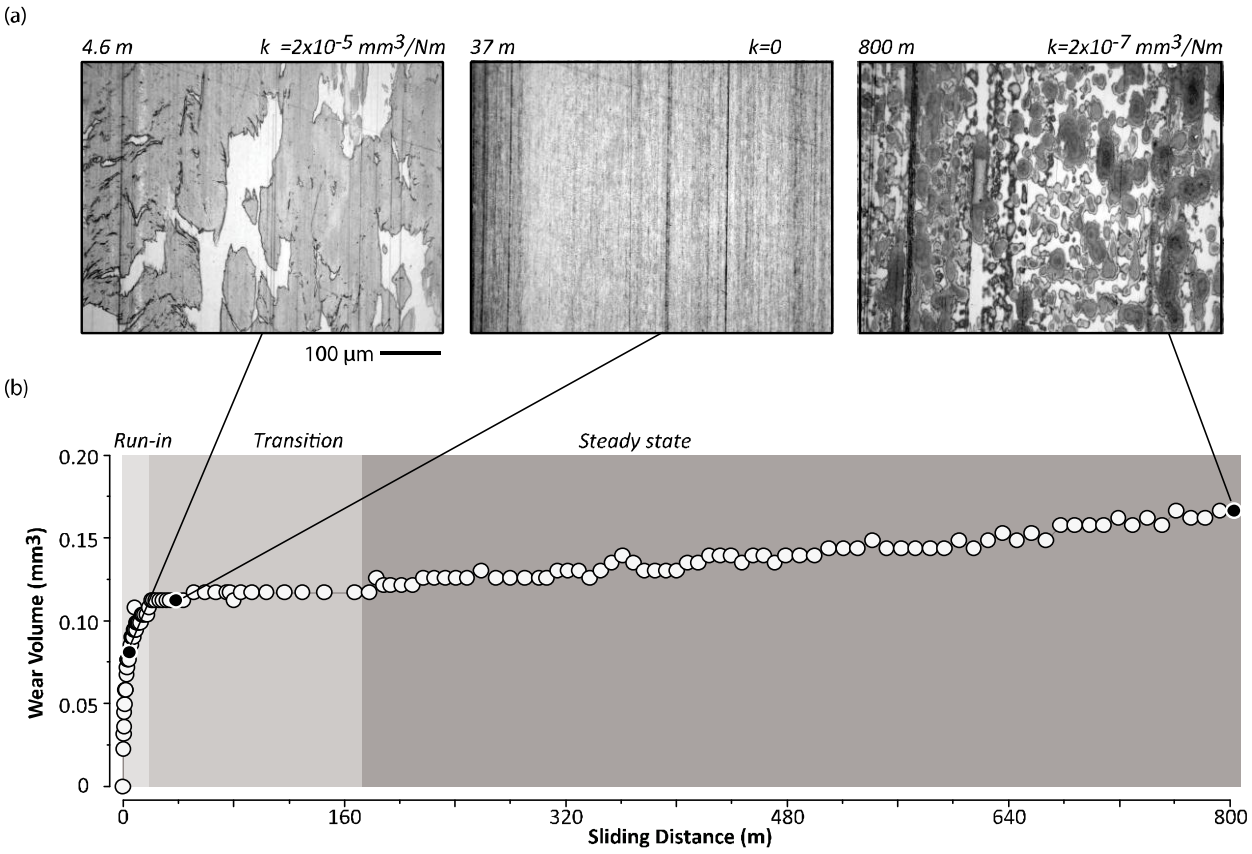

Figure 6. (a) Representative images of the transfer film morphology for the ***run-in***, ***transition***, and ***steady-state*** phases. The stainless counterface appears bright. (b) Wear volume is plotted versus distance for the first 800 m of sliding. The images correspond to the black data labels. Each image has the scale shown.

Based on these results, it was hypothesized that the mechanism responsible for reinforcing the interface was similar to the mechanism responsible for reinforcing a composite. In other words, the transfer film is least effective when the exposed regions are characteristically large and is most effective when the exposed regions are characteristically small; it has already been shown that wear rate is independent of film coverage fraction [39]. The dispersion characterization code was used here to characterize the free-space length of the uncoated areas of the transfer film. Figure 7 illustrates the calculation of the free-space length, L_f, for the alumina-PTFE nanocomposite. First the optical image from the interrupted experiment is converted to black and white as before. The code then runs the iterative procedure to determine L_f, which, in this case is 13.5µm.

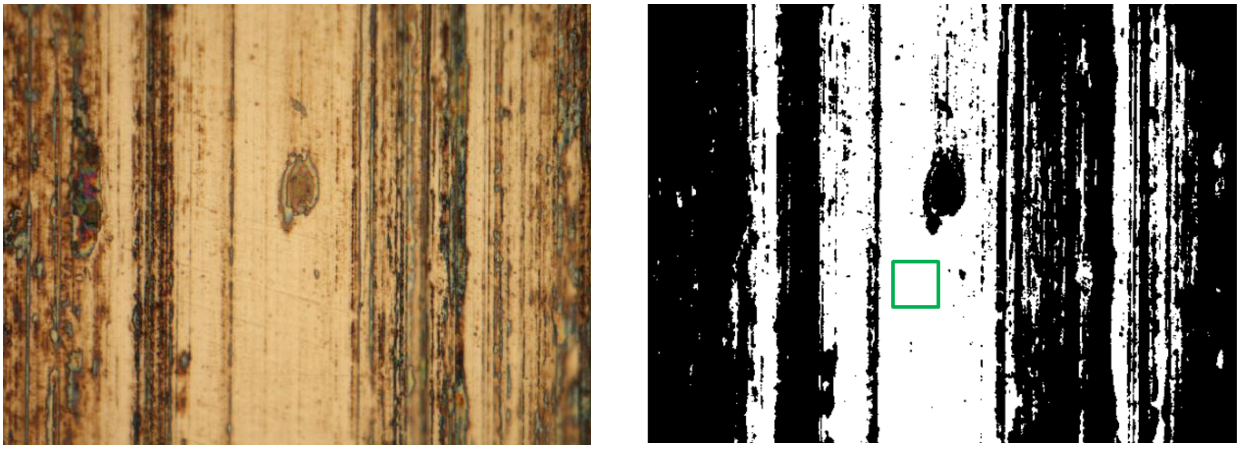

Figure 7. Left) optical image of a transfer film. Right) Conversion of the optical image to black and white. The free-space length for this particular image, illustrated by the green square, is 13.5µm.

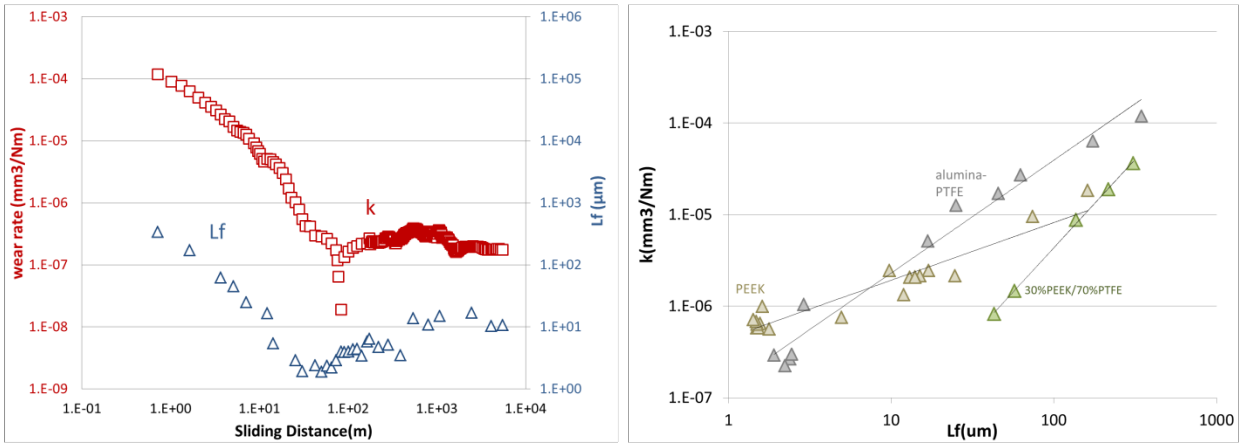

Figure 8. Left) wear rate and free-space length plotted versus sliding distance for the alumina-PTFE nanocomposite system. The free-space length, L_f, correlates strongly with the wear rate of the system, with both equalizing at steady-state. Right) wear rate versus L_f for alumina-PTFE, unfilled PEEK, and 30%PEEK-PTFE. In each case, the wear rate obeys a power law relationship with L_f. Higher powers yield higher potential for wear reduction and is likely driven by constituent properties.

Wear rate is correlated to free-space length for several independent polymer systems in Figure 8. The free-space length, L_f, clearly correlates strongly with the wear rate. In each case, the wear rate obeys a power law relationship with L_f. Higher powers yield higher potential for wear reduction and is likely driven by constituent properties

3.2.2 Tribology

Tribo-films are inherently nanostructured. To probe the properties of these films, extremely small contact forces and areas are required. The only available instrument capable of friction coefficient measurements of sufficient resolution to probe the top 10 nm is the atomic force microscope (AFM). Unfortunately, while there are accepted methods for accurately quantifying AFM normal force, calibrating the friction force signals from the instrument is notoriously difficult. To date, no one calibration method has been adopted by the community due to a lack of accuracy, simplicity, traceability, or general applicability. The goal here was to develop a simple in-situ method of lateral force calibration that: (1) allows simultaneous calibration and measurement, thus eliminating prior tip damage, confounding effects of instrument setup adjustments, and the requirement of special calibration substrates; (2) is insensitive to adhesion, PSD cross talk, transducer/piezo-tube axis misalignment, and shear-center offset; (3) is applicable to integrated tips and colloidal probes; (4) is generally applicable to any reciprocating friction coefficient measurement.

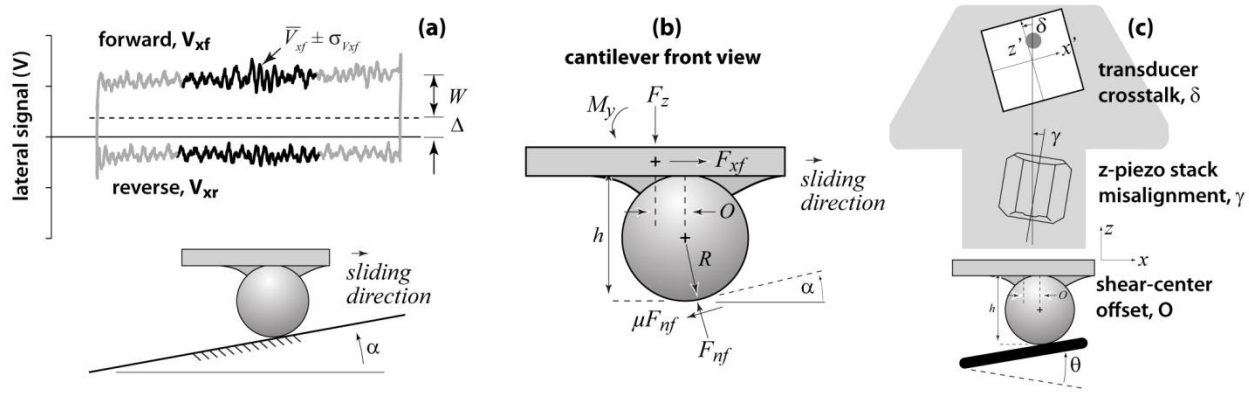

Figure 9. **(a)** Illustration of the friction loop resulting from sliding on a flat tilted substrate and definitions of the experimental friction loop offset, *Δ*, and the friction loop half-width, *W*, as defined in Ogletree *et al*. [40]. **(b)** Free-body diagram of the tip during forward sliding against a wedge of angle α, where α is the angle of the surface relative to the cantilever x-axis. The tip is offset from the centroidal axis (shear center) of the cantilever by a distance O (cantilever extends into the plane of paper) **(c)** Illustration of the model AFM used in the calibration analysis; transducer cross-talk, piezo-tilt and tip-offset are considered; θ=α+γ.

The "wedge-method" is among the most robust and widely used method of lateral force calibration. However, it does not explicitly account for offset in shear-center (tip-offset) or finite probe radius, both of which can cause large uncertainty. This work replicates the wedge method, but starts with a model that does explicitly account for tip-offset, *O*, and finite probe radius, *R*, as illustrated in Figure 9. According to the wedge method, by measuring vertical and lateral voltages during sliding on two different sloped substrates, a unique calibration constant can be determined if the relative angel between slopes is known. With this more complicated model, there exist two more unknowns than equations, precluding explicit determination of a unique

calibration constant. Manufacturers report probe radii and cantilever geometry, which eliminates one unknown. By using these reported estimates with γ=0, it was shown that calibration constants can be solved for with uncertainties an order of magnitude smaller than typical statistical fluctuations for γ<45°.

3.3 Environmental Tribometry

3.3.1 Macrotribology

Tribology is driven by mechanics and chemistry. Molybdenum disulfide tribology is particularly sensitive to chemistry, but the mechanisms involved are current topics of debate. For example, the friction of MoS_2 at room temperature increases dramatically when it is exposed to water, but is unaffected by oxygen [41]. Interestingly, the sensitivity to water has been attributed to preferential oxidation by water over oxygen [42-53]. However, numerous recent studies have shown that significant oxidation only occurs at relatively high temperatures, and is driven by oxygen not water [54-59]. The goal here was to elucidate the mechanism of environmental sensitivity by conducting a full systematic study of MoS_2 friction under controlled environment and temperature conditions.

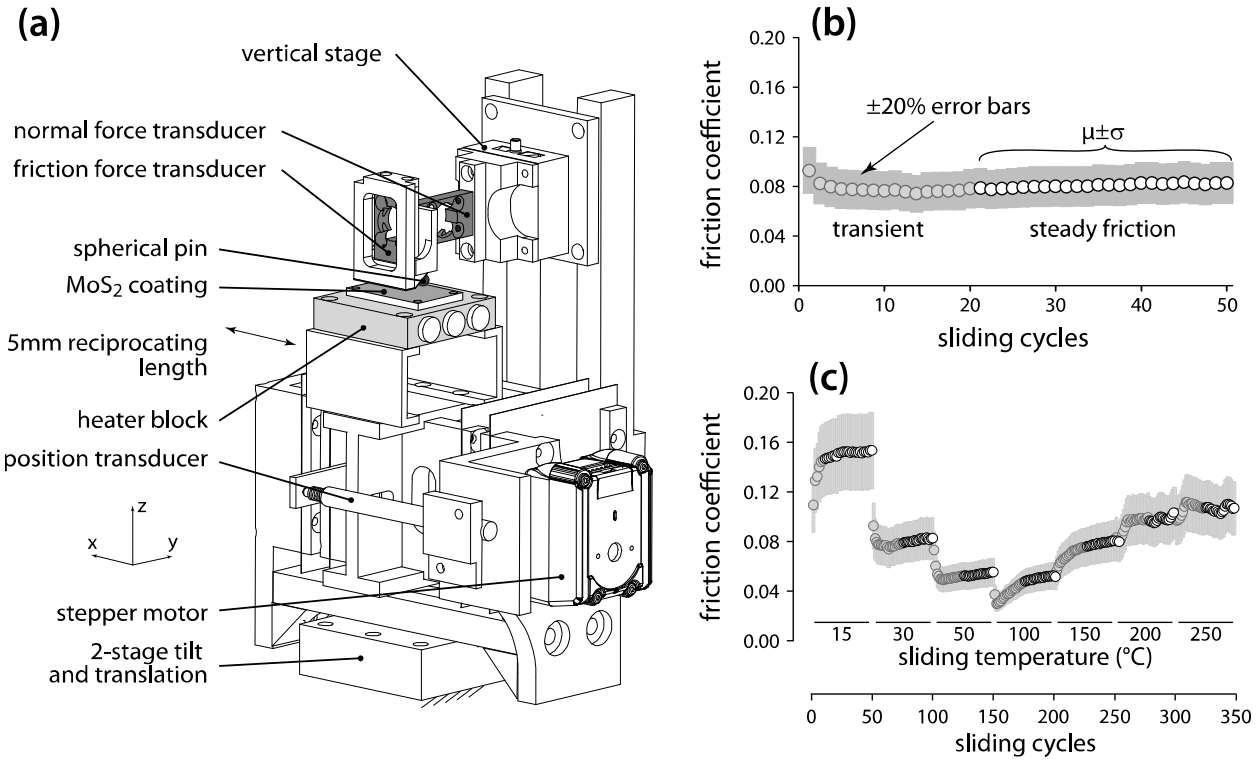

Figure 10. (a) Schematic illustration of the custom high temperature tribometer with a reciprocating pin-on-flat contact. A stepper motor drives the reciprocating motion in the x-axis for a given track length and sliding frequency. Contact forces are measured by two strain-gage-based transducers connected to a manual vertical stage, used for loading the contact. A heater block with cartridge heater inserts is connected to a PID temperature controller; the tribometer and data acquisition hardware is housed in a glove box for environmental control. (b) Friction coefficients were calculated using values from the final 30 sliding cycles (grey markers), where variations in friction

between sliding cycles were observed to be below 20% (grey error bars). (b) Friction coefficients at elevated temperatures also showed a steady state behavior toward the last 30 of 50 sliding cycles.

Sliding tests were conducted on the custom-built, pin-on-flat reciprocating tribometer illustrated in Figure 10. The linear reciprocating stage of the tribometer is driven along the x-axis by a stepper motor (via a lead screw and flexure assembly) interfaced to a computer running LabView™ for motion control. MoS_2 samples were mounted to a copper heater block containing cartridge heater inserts. A surface mounted thermocouple provided feedback to a PID temperature controller. MoS_2 coatings were mounted directly to the heater. The heater block was attached to the linear stage via two C-section brackets that were designed to minimize conduction into the stage. Two strain gage load cells (Strain Measurement Devices) measured the normal and friction force and were rigidly attached to a manual dovetail linear stage which was used for loading and unloading the contact in the z-direction. The load cells were calibrated with a Mettler mass balance with an uncertainty of 50µg; the overall force uncertainty in the calibration of the load cells was 0.1mN. A thin aluminum cantilever separated the load cell assembly from the tribological contact, which enabled the load cell assembly to remain at 27°C±3°C under all thermal conditions. The variable temperature tribometer was housed within an environmental glovebox which allowed independent control over the environmental constituents.

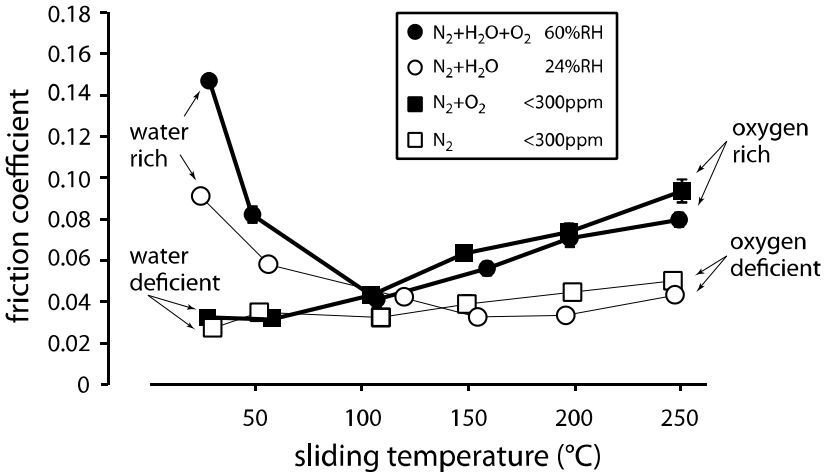

Figure 11. Friction of conditioned sputtered MoS_2 coatings in dry nitrogen, dry air, humid nitrogen, and humid air as a function of temperature. Water increases friction at low temperatures with or without oxygen. Oxygen increases friction at high temperature with or without water.

The friction coefficient of MoS_2 is shown in Figure 11 as a function of temperature and environment. Friction increased at room temperature when water was present regardless of whether oxygen was present; this is consistent with previous findings [44, 46]. However, the trend was reversed at 250°C, where friction increased with the presence of oxygen regardless of whether water was present; these were the first measurements of this trend. Interestingly, the water-free environment had slightly higher friction at this temperature. Variable humidity studies showed a statistically significant reduction in the high temperature friction when water

content increased. The addition of water and oxygen to nitrogen significantly increased friction at low and high temperatures; the temperature at which friction is minimized is called the transition temperature. All four environmental conditions produced nominally identical friction coefficients at the transition temperature. In this case, the transition temperature occurred at 100°C which corresponds to the temperature at which Windom *et al.* [58] first observed increased oxidation and Kubart *et al.* [55] first observed increased friction. These results suggest that water drives increased friction coefficients below the transition temperature and oxygen drives increased friction coefficients above the transition temperature.

EDS measurements of oxygen content (O Kα) were made to assess the possible role of oxidation in determining frictional transitions in varying environmental conditions. The coating was worn at room temperature in dry N_2 to remove native surface oxides and worn track was treated as the reference datum for oxidation. The data for the worn and unworn coating for this condition are shown in white labels in Figure 12; the statistical 95% confidence intervals are denoted by the shaded region. It is clear that sliding in nitrogen at room temperature removed a significant amount of oxygen from the surface; the surface was presumably oxidized by exposure to thermal cycling in varying environments throughout the study. Annealing the coating at 250°C in dry N_2 did not increase oxygen content in the worn area; in fact, there was a statistically significant reduction in oxygen content that we believe to be due to water desorption. Annealing in humid N_2 had no effect on oxygen inside or outside the worn area; this suggests that water does not promote oxidation within the detection limits of EDS. In contrast, dry air annealing significantly increased O Kα. The annealing step did not affect oxygen content outside the wear track under any condition suggesting that this is an oxide equilibrium state for temperatures below 250°C. The EDS results suggest that only oxygen causes significant oxidation and only high temperatures. This suggests that water affects the friction of MoS_2 directly, through non-oxidative routes.

The trend of decreased friction with increased temperature in humid environments at temperatures below the transition can be explained by thermally activated slip or thermally activated desorption. Annealing experiments were conducted to isolate these contributions (Figure 13). Coatings were conditioned in lab air for a day prior and annealed by heating the sample to various temperatures for various times. Friction coefficients were then measured in air at room temperature. Annealing the coating at 50°C, for example, decreased the room temperature friction; this reduction cannot be due to thermally activated slip since the interface temperature, which drives thermally activated slip, is unchanged. Thus, thermally activated desorption must be primarily responsible for decreased friction with increased temperature. The nature of the bonds must be physical since chemically bound water desorbs at 370°C [60]. Finally, the results demonstrate that subsurface adsorption and diffusion play major roles in determining friction. These samples were exposed to air during cooling for substantial periods (~15 min) prior to testing at room temperature. Surface adsorption occurs on much shorter time scales and would have equilibrated well before the friction experiment began. Thermally

activated desorption explains why friction generally reduces with increased temperature at temperatures below the transition to oxidation.

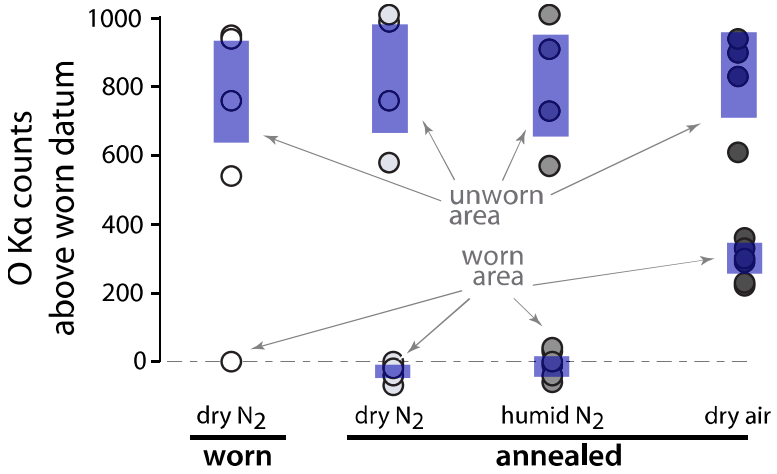

Figure 12. EDS O Kα values measured on the unworn and worn MoS_2 coating after annealing in different environments. Measurements were made at six locations within the track and four locations outside the track (on the unworn coating). Wear in dry nitrogen significantly reduced the oxygen content of the worn region. Only annealing in dry air caused a significant increase in the oxygen content in the worn area, suggesting that oxygen is more effective than water at oxidizing MoS_2.

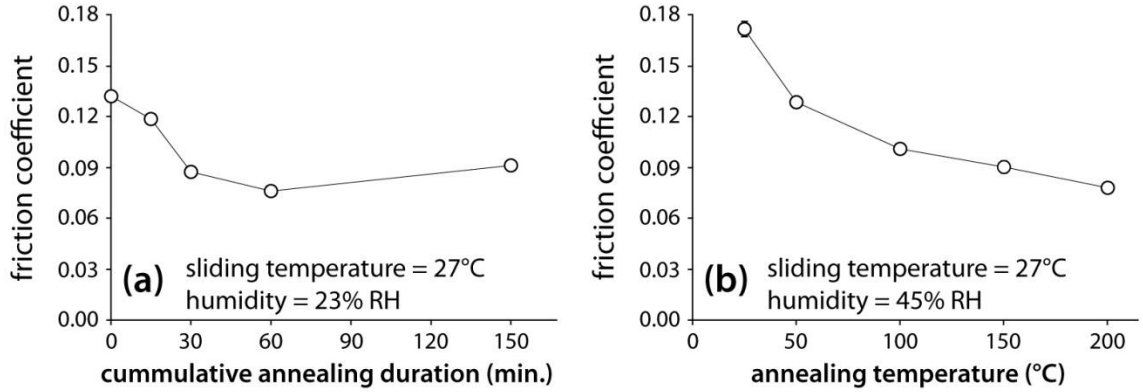

Figure 13. (a) In fixed-temperature annealing experiment, MoS_2 coating was annealed to 110°C for 15, 15, 30 and 90 minutes in humid air (23% RH) (b) In fixed-time anneal, coating was heated for 20 minutes each at 50°C, 100°C, 150°C and 200°C in humid air (45% RH). Friction measured in humid air at 30°C between subsequent anneals shows gradual reduction with increased duration of thermal conditioning for both experiments, suggesting the desorption of diffused water.

These results were used to develop a model hypothesis for the environmental sensitivity of MoS_2 tribology. The model is illustrated in Figure 14 and forms the basis of the experimental design used in this study. The presence of water and oxides (not oxygen itself) directly impedes inter-lamellar shear and thereby directly increases friction. Oxidation is surface (or near-surface) limited while water (hydration) can diffuse into the bulk. Increased time at increased temperature in oxidizing environments increases the concentration of near surface oxides while

wear reduces them. Increased time in humid environments increases hydration while heating the coating reduces hydration.

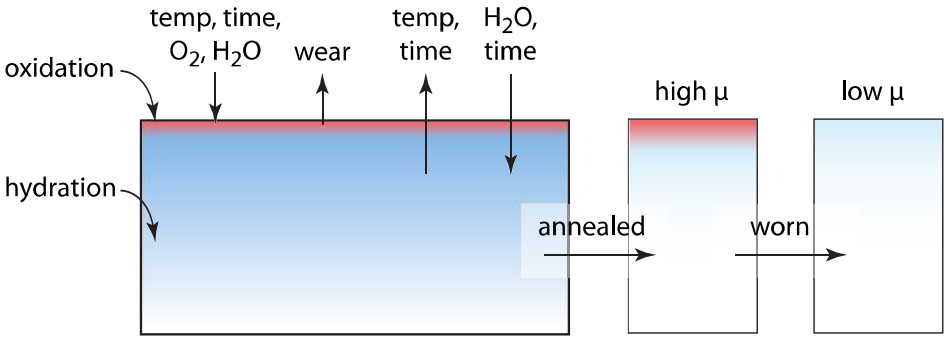

Figure 14. Schematic illustration of the hypothesis being investigated in this study. Oxidation (surface limited) is shown in red and hydration (diffused) is shown in blue. Increased time, temperature, oxygen and water increase the rate, concentration, and depth of surface oxidation. Wear actively removes oxides. Increased time and temperature with reduced environmental moisture reduces the water content of the coating. Annealing is a heating step (to variable temperatures for varying time) used to drive off water in the coating; this step causes further oxidation. Sliding wear can be used to scrub off the oxidized surface.

3.3.2 Nanotribology

The calibration methods described in 3.2.2 have been used to characterize the nanotribological properties of several systems of interest including various forms of MoS_2. Calibrated friction data for single crystal MoS_2 and graphitic carbon sliding against an integrated Si tip in room temperature air are shown in Figure 15 to illustrate material-driven differences in friction. The method is used to determine the friction forces corresponding to a range of normal force. The friction coefficient is the best linear fit to the data. The nanoscale friction coefficient of graphitic carbon (μ=0.2) is consistent with the macroscale friction coefficient. The nanoscale friction coefficient of single crystal MoS_2 was orders of magnitude lower than was observed for sputtered films at the macroscale (*e.g.* Figure 11). In each case analyzed, uncertainty was due to statistical fluctuations in the actual friction coefficients (error bars), not uncertainty from the calibration method itself.

Using the same calibration method, the effect of storage environment on nanoscale friction was quantified on different substrates, as shown in Figure 16 (left). Repeat measurements were made on four consecutive days on polished aluminum, MoS_2, graphitic carbon and HOPG in random testing order to assess variability and potential effects of transfer. The measurements demonstrate significant and repeatable substrate material-driven variations in friction covering several orders of magnitude. Of all the measurements, only the first measurement of graphitic carbon appeared as an outlier. This likely resulted from tip contamination by a previous measurement. In sum, the friction coefficient is surprisingly insensitive to the material previously tested. This suggests that the nanoscale measurements do discourage wear and transfer. This was supported by the lack of evidence of wear during topography scans taken directly after friction characterization.

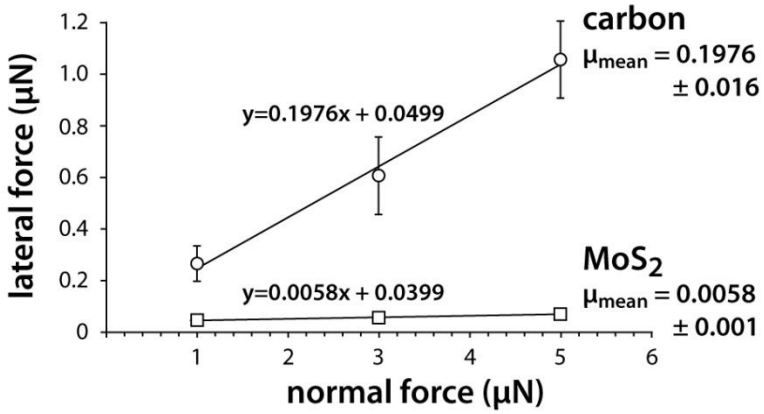

Figure 15. Calibrated lateral force versus normal force for AFM measurements of carbon and single crystal MoS_2 with integrated Si probes. Colloidal probe measurements on MoS_2 would overlap the integrated data points and would not be distinguishable. Slightly different mean friction coefficients and smaller standard errors were obtained with a linear fit of calibrated force data compared to those from the calibration method itself.

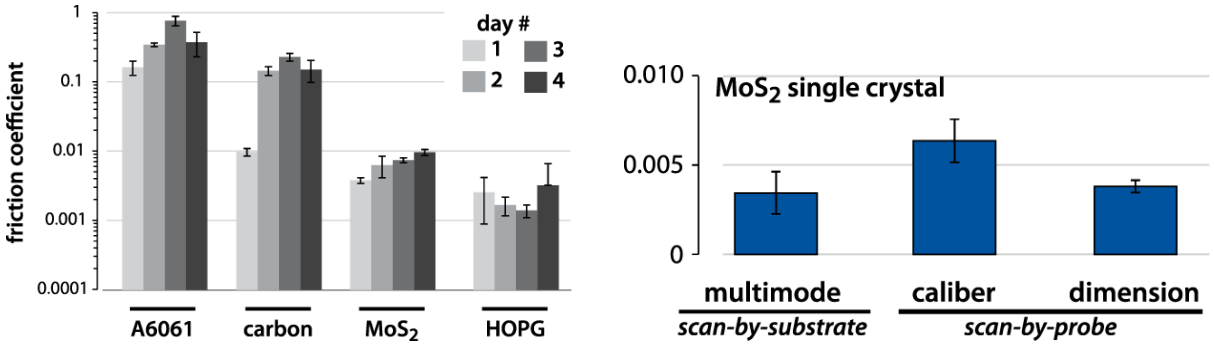

Figure 16. Left) Calibrated friction coefficients for an integrated Si AFM tip sliding against various materials in air over several days of testing. Test order was randomized to capture potential effects of material transfer. The consistency suggests that test ordering and tip contamination did not significantly affect friction. **Right)** Calibrated friction coefficient for single crystal MoS_2 measured by three different AFM systems. The calibration method and tribological results are not sensitive to the AFM system, despite major differences in design.

A truly quantitative calibration method will yield the same results under the same conditions on different instruments. This type of instrument-driven frictional variation is a general problem in tribology and has motivated efforts to develop more robust methods to reduce measurement uncertainties [61], which can be large fractions of the measured friction coefficient. These instrument driven variations were evaluated by performing friction measurements on three different AFM platforms with significant design differences. Each instrument reported friction coefficients in the range from μ=0.003-0.007 in air, values that are clearly within the day to day repeatability shown on the left of Figure 16.

One of the primary hypotheses for this research was that nanoscale structure was a primary contributor to the friction reduction mechanism of tribofilms. This effect was investigated by measuring nanoscale friction coefficients on MoS_2 surfaces of varying order; unworn sputtered surfaces had no tribofilms, worn sputtered surfaces had tribofilms, and single crystal MoS_2 was

used as the structural control. Measurements were made across the surfaces to capture spatial variations in friction, driven either by microstructure or roughness. As shown in Figure 17, the presence of sliding-induced tribofilms significantly reduced friction in humid and dry environment. The tribofilm was nearly uniform across the wear scar as evidenced by the reduction in the standard deviation relative to unworn coating. Friction measured on the ideal, basally-oriented single crystal structure was reduced further. It appears that the tribofilm approaches the ideal structure during sliding; higher friction of the tribofilm is likely due more to the more frequent presence of edge-sites than to a lack of basal orientation. Additionally, the results illustrate that water increases friction in every case. Finally, the results demonstrate significantly reduced friction at the nanoscale than the microscale, especially in the humid environment. Although the cause is uncertain, it is likely related to bulk deformations and their effects on friction.

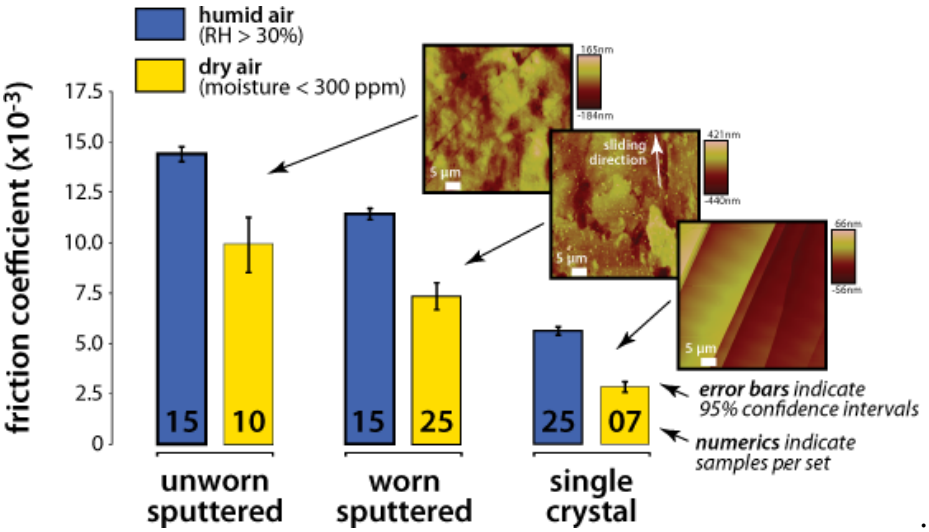

Figure 17. Left) Calibrated friction coefficients for an integrated Si AFM tip sliding against various materials in air over several days of testing. Test order was randomized to capture potential effects of material transfer. The consistency suggests that test ordering and tip contamination did not significantly affect friction.

4.0 Closing

The overall goal of the work was to interrogate the tribological, morphological, and mechanical evolutions of surfaces to elucidate their relationships during sliding. This project successfully developed several enabling tools for characterizing nanoparticle dispersion, transfer film morphology, nanoscale friction coefficients, and variable environment testing. These efforts enabled improved understanding of 1) the effects of processing on nanocomposite performance, 2) the formation mechanisms of transfer films and their role in wear resistance, 3) the role of water and oxygen in increased friction of MoS_2, and 4) size-scale effects on friction.

References

[1] Astrene, T., 2004, "20 Minutes With...Walt Musial," Tribology and Lubrication Technology, pp. 26-34.

[2] Musial, W., and Butterfield, S., 2007, "Improving Wind Turbine Gearbox Reliability," National Renewable Energy Laboratory, Boulder, CO USA.

[3] De Groh, K. K., Banks, B. A., McCarthy, C. E., Rucker, R. N., Roberts, L. M., and Berger, L. A., 2008, "MISSE 2 PEACE polymers atomic oxygen erosion experiment on the International Space Station," High Performance Polymers, 20(4-5), pp. 388-409.

[4] Dever, J. A., Miller, S. K., Sechkar, E. A., and Wittberg, T. N., 2008, "Space environment exposure of polymer films on the materials international space station experiment: Results from MISSE 1 and MISSE 2," High Performance Polymers, 20(4-5), pp. 371-387.

[5] Bowden, F. P., and Rowe, G. W., 1956, "The Adhesion of Clean Metals," PROC R SOC LON SER-A, 233(1195), pp. 429-442.

[6] Miyoshi, K., 1999, "Aerospace mechanisms and tribology technology - Case study," TRIBOL INT, 32(11), pp. 673-685.

[7] Lavik, M., Haltner, A. J., and Spalvins, T., 1969, "Discussion of Deposition of Mos2 Films by Physical Sputtering and Their Lubrication Properties in Vacuum," Asle Transactions, 12(1), pp. 41-&.

[8] Voevodin, A. A., Fitz, T. A., Hu, J. J., and Zabinski, J. S., 2002, "Nanocomposite tribological coatings with "chameleon" surface adaptation," Journal of Vacuum Science & Technology a-Vacuum Surfaces and Films, 20(4), pp. 1434-1444.

[9] Voevodin, A. A., Hu, J. J., Fitz, T. A., and Zabinski, J. S., 2001, "Tribological properties of adaptive nanocomposite coatings made of yttria stabilized zirconia and gold," Surface & Coatings Technology, 146, pp. 351-356.

[10] Voevodin, A. A., and Zabinski, J. S., 2005, "Nanocomposite and nanostructured tribological materials for space applications," Composites Science and Technology, 65(5), pp. 741-748.

[11] Voevodin, A. A., and Zabinski, J. S., 2006, "Laser surface texturing for adaptive solid lubrication," Wear, 261(11-12), pp. 1285-1292.

[12] Voevodin, A. A., Zabinski, J. S., and Muratore, C., 2005, "Recent advances in hard, tough, and low friction nanocomposite coatings," Tsinghua Science and Technology, 10(6), pp. 665-679.

[13] Zabinski, J. S., Donley, M. S., Walck, S. D., Schneider, T. R., and Mcdevitt, N. T., 1995, "The Effects of Dopants on the Chemistry and Tribology of Sputter-Deposited Mos2 Films," Tribology Transactions, 38(4), pp. 894-904.

[14] Bahadur, S., and Tabor, D., 1984, "The Wear of Filled Polytetrafluoroethylene," WEAR, 98(1-3), pp. 1-13.

[15] Blanchet, T., and Kennedy, F., 1992, "Sliding Wear Mechanism of Polytetrafluoroethylene (PTFE) and PTFE Composites," WEAR, 153(1), pp. 229-243.

[16] Burris, D., and Sawyer, W., 2006, "Improved wear resistance in alumina-PTFE nanocomposites with irregular shaped nanoparticles," WEAR, 260(7-8), pp. 915-918.

[17] Burris, D., and Sawyer, W., 2006, "A low friction and ultra low wear rate PEEK/PTFE composite," WEAR, 261(3-4), pp. 410-418.

[18] Bahadur, S., and Polineni, V., 1996, "Tribological studies of glass fabric-reinforced polyamide composites filled with CuO and PTFE," WEAR, 200(1-2), pp. 95-104.

[19] Muratore, C., Hu, J. J., and Voevodin, A. A., 2007, "Adaptive nanocomposite coatings with a titanium nitride diffusion barrier mask for high-temperature tribological applications," Thin Solid Films, 515(7-8), pp. 3638-3643.

[20] Muratore, C., and Voevodin, A. A., 2006, "Molybdenum disulfide as a lubricant and catalyst in adaptive nanocomposite coatings," Surface & Coatings Technology, 201(7), pp. 4125-4130.

[21] Muratore, C., Voevodin, A. A., Hu, J. J., and Zabinski, J. S., 2006, "Tribology of adaptive nanocomposite yttria-stabilized zirconia coatings containing silver and molybdenum from 25 to 700 degrees C," Wear, 261(7-8), pp. 797-805.

[22] Muratore, C., Voevodin, A. A., Hu, J. J., and Zabinski, J. S., 2006, "Multilayered YSZ-Ag-Mo/TiN adaptive tribological nanocomposite coatings," Tribology Letters, 24(3), pp. 201-206.

[23] Voevodin, A. A., O'Neill, J. P., and Zabinski, J. S., 1999, "Nanocomposite tribological coatings for aerospace applications," Surface & Coatings Technology, 119, pp. 36-45.

[24] Archard, J. F., and Hirst, W., 1957, "An Examination of a Mild Wear Process," PROC R SOC LON SER-A, 238(1215), pp. 515-&.

[25] Hu, J. J., Wheeler, R., Zabinski, J. S., Shade, P. A., Shiveley, A., and Voevodin, A. A., 2008, "Transmission Electron Microscopy Analysis of Mo–W–S–Se Film Sliding Contact Obtained by Using Focused Ion Beam Microscope and In Situ Microtribometer " Tribology Letters, 32(1), pp. 49-57.

[26] Scharf, T. W., and Singer, I. L., 2003, "Monitoring transfer films and friction instabilities with in situ Raman tribometry," TRIBOL LETT, 14(1), pp. 3-8.

[27] Scharf, T. W., and Singer, I. L., 2002, "Role of third bodies in friction behavior of diamond-like nanocomposite coatings studied by in situ tribometry," TRIBOL T, 45(3), pp. 363-371.

[28] Wahl, K. J., Chromik, R. R., and Lee, G. Y., 2008, "Quantitative in situ measurement of transfer film thickness by a Newton's rings method," WEAR, 264(7-8), pp. 731-736.

[29] McCook, N., Burris, D., Bourne, G., Steffens, J., Hanrahan, J., and Sawyer, W., 2005, "Wear resistant solid lubricant coating made from PTFE and epoxy," TRIBOL LETT, 18(1), pp. 119-124.

[30] Jang, I., Burris, D. L., Dickrell, P. L., Barry, P. R., Santos, C., Perry, S. S., Phillpot, S. R., Sinnott, S. B., and Sawyer, W. G., 2007, "Sliding orientation effects on the tribological properties of polytetrafluoroethylene," Journal of Applied Physics, 102.

[31] Beamson, G., Clark, D., Deegan, D., Hayes, N., Law, D., Rasmusson, J., and Salaneck, W., 1996, "Characterization of PTFE on silicon wafer tribological transfer films by XPS, imaging XPS and AFM," SURF INTERFACE ANAL, 24(3), pp. 204-&.

[32] Breiby, D., Solling, T., Bunk, O., Nyberg, R., Norrman, K., and Nielsen, M., 2005, "Structural surprises in friction-deposited films of poly(tetrafluoroethylene)," MACROMOLECULES, 38(6), pp. 2383-2390.

[33] MAKINSON, K., and TABOR, D., 1964, "FRICTION + TRANSFER OF POLYTETRAFLUOROETHYLENE," NATURE, 201(491), pp. 464-&.

[34] POOLEY, C., and TABOR, D., 1972, "FRICTION AND MOLECULAR STRUCTURE - BEHAVIOR OF SOME THERMOPLASTICS," PROC R SOC LON SER-A, 329(1578), pp. 251-&.

[35] Burris, D. L., Santos, K., Lewis, S. L., Liu, X., Perry, S. S., Blanchet, T., Schadler, L., and Sawyer, W. G., 2008, "Polytetrafluoroethylene Matrix Nanocomposites for Tribological Applications," Tribology of Polymeric Nanocomposites, K. Friedrich, ed.

[36] Burris, D. L., Zhao, S., Duncan, R., Lowitz, J., Perry, S. S., Schadler, L. S., and Sawyer, W. G., 2009, "A route to wear resistant PTFE via trace loadings of functionalized nanofillers," WEAR, 267(1-4), pp. 653-660.

[37] Burris, D. L., Boesl, B., Bourne, G. R., and Sawyer, W. G., 2007, "Polymeric nanocomposites for tribological applications," Macromolecular Materials and Engineering, 292(4), pp. 387-402.

[38] Ye, J., Khare, H. S., and Burris, D. L., 2013, "Transfer film evolution and its role in promoting ultra-low wear of a PTFE nanocomposite," WEAR, 297(1-2), pp. 1095-1102.

[39] Laux, K. A., and Schwartz, C. J., 2013, "Effects of contact pressure, molecular weight, and supplier on the wear behavior and transfer film of polyetheretherketone (PEEK)," WEAR, 297(1-2), pp. 919-925.

[40] Ogletree, D. F., Carpick, R. W., and Salmeron, M., 1996, "Calibration of frictional forces in atomic force microscopy," Review of Scientific Instruments, 67(9), pp. 3298-3306.

[41] Donnet, C., Martin, J. M., LeMogne, T., and Belin, M., 1996, "Super-low friction of MoS2 coatings in various environments," Tribology International, 29(2), pp. 123-128.

[42] Stewart, T. B., and Fleischauer, P. D., 1982, "Chemistry of Sputtered Molybdenum-Disulfide Films," Inorganic Chemistry, 21(6), pp. 2426-2431.

[43] Degee, A. W. J., Salomon, G., and Zaat, J. H., 1965, "On Mechanisms of Mos2-Film Failure in Sliding Friction," Asle Transactions, 8(2), pp. 156-163.

[44] Dudder, G., Zhao, X., Krick, B., Sawyer, W. G., and Perry, S., 2011, "Environmental Effects on the Tribology and Microstructure of MoS2-Sb2O3-C Films," Tribology Letters, 42(2), pp. 203-213.

[45] Fleischauer, P. D., and Lince, J. R., 1999, "A comparison of oxidation and oxygen substitution in MoS2 solid film lubricants," Tribology International, 32(11), pp. 627-636.

[46] Fusaro, R. L., 1978, "Lubrication and Failure Mechanism of Molybdenum Disulfide Films. I. Effect of Atmosphere," NASA, Cleveland, OH.

[47] Haltner, A. J., and Oliver, C. S., 1966, "Effect of Water Vapor on Friction of Molybdenum Disulfide," Industrial & Engineering Chemistry Fundamentals, 5(3), pp. 348-355.

[48] Panitz, J. K. G., Pope, L. E., Lyons, J. E., and Staley, D. J., 1988, "The Tribological Properties of Mos2 Coatings in Vacuum, Low Relative-Humidity, and High Relative-Humidity Environments," Journal of Vacuum Science & Technology a-Vacuum Surfaces and Films, 6(3), pp. 1166-1170.

[49] Pardee, R. P., 1972, "Effect of Humidity on Low-Load Frictional Properties of a Bonded Solid Film Lubricant," Asle Transactions, 15(2), pp. 130-142.

[50] Salomon, G., De Gee, A. W. J., and Zaat, J. H., 1964, "Mechano-chemical factors in MoS2-film lubrication," Wear, 7(1), pp. 87-101.

[51] Cannon, P., and Norton, F. J., 1964, "Reaction between Molybdenum Disulphide and Water," Nature, 203(494), pp. 750-751.

[52] Fleischauer, P. D., 1984, "Effects of Crystallite Orientation on Environmental Stability and Lubrication Properties of Sputtered Mos2 Thin-Films," Asle Transactions, 27(1), pp. 82-88.

[53] Ross, S., and Sussman, A., 1955, "Surface Oxidation of Molybdenum Disulfide," Journal of Physical Chemistry, 59(9), pp. 889-892.

[54] Sliney, H. E., 1974, "High-Temperature Solid Lubricants .1. Layer Lattice Compounds and Graphite," Mechanical Engineering, 96(2), pp. 18-22.

[55] Kubart, T., Polcar, T., Kopecky, L., Novak, R., and Novakova, D., 2005, "Temperature dependence of tribological properties of MoS(2) and MoSe(2) coatings," Surface & Coatings Technology, 193(1-3), pp. 230-233.

[56] Lansdown, A. R., 1999, Molybdenum disulphide lubrication, Elsevier, Amsterdam.

[57] Godfrey, N. a. N., E.C., 1949, "Oxidation Characteristics of Molybdenum Disulfide and Effect of Such Oxidation on its Role as a Solid Film Lubricant," NACA TN No. 1882.

[58] Windom, B. C., Sawyer, W. G., and Hahn, D. W., 2011, "A Raman Spectroscopic Study of MoS(2) and MoO(3): Applications to Tribological Systems," Tribology Letters, 42(3), pp. 301-310.

[59] Muratore, C., Bultman, J. E., Aouadi, S. M., and Voevodin, A. A., 2011, "In situ Raman spectroscopy for examination of high temperature tribological processes," Wear, 270(3-4), pp. 140-145.

[60] Pierce, D. E., Burns, R. P., Dauplaise, H. M., and Mizerka, L. J., 1991, "Thermal-Desorption Spectroscopy of Sputtered Mosx Films," Tribology Transactions, 34(2), pp. 205-214.

[61] Burris, D. L., and Sawyer, W. G., 2009, "Addressing Practical Challenges of Low Friction Coefficient Measurements," TRIBOL LETT, 35(1), pp. 17-23.